frontiers | Frontiers in Materials

TYPE Original Research
PUBLISHED 06 September 2024
DOI 10.3389/fmats.2024.1367754

OPEN ACCESS

EDITED BY
Di Zhou,
Xi'an Jiaotong University, China

REVIEWED BY
Charanjeet Singh,
Lovely Professional University, India
Guoguang Yao,
Xian University of Posts and Telecommunication, China

*CORRESPONDENCE
Ashwini Kumar,
kumar1984@lzy.edu.cn

RECEIVED 09 January 2024
ACCEPTED 12 July 2024
PUBLISHED 06 September 2024

CITATION
Kumar A, Sharma P and Qiu F (2024), Structure characteristics and microwave dielectric properties of $ZnZrNb_2O_8$ oxide ceramics. *Front. Mater.* 11:1367754.
doi: 10.3389/fmats.2024.1367754

Structure characteristics and microwave dielectric properties of $ZnZrNb_2O_8$ oxide ceramics

Ashwini Kumar*, Poorva Sharma and Fujun Qiu

Luzhou Key Laboratory of Intelligent Control and Application Technology of Electronic Devices, School of Electrical and Electronics Engineering, Luzhou Vocational and Technical College, Luzhou, Sichuan, China

This study investigates the synthesis, structural analysis, and microwave dielectric characteristics of $ZnZrNb_2O_8$ ceramics, prepared via solid-state reaction method and subjected to sintering at temperatures ranging from 1,000°C to 1,200°C for 4 h. X-ray diffraction (XRD) analysis confirms the successful formation of $ZnZrNb_2O_8$ phase, with a monoclinic wolframite phase. Scanning electron microscopy (SEM) investigations unveil microstructural features such as grain size and porosity, reveals material's morphological details. Dielectric properties conducted in the microwave frequency regime show a correlation between dielectric constant (ε_r) and relative density of the ceramics. Importantly, the ceramics exhibited a suitable dielectric constant and low dielectric loss, indicative of their suitability for microwave applications. Remarkably, $ZnZrNb_2O_8$ ceramics sintered at 1,150°C for 4 h exhibit excellent microwave dielectric properties (ε_r = 27.2, $Q \times f$ = 54,500 GHz, and τ_f = −60 ppm/°C). These findings underscore the potential of $ZnZrNb_2O_8$ ceramics as advanced materials for high-frequency applications, including filters, resonators, and other microwave devices, thus contributing significantly to the advancement of next-generation telecommunications technologies.

KEYWORDS

ceramics, crystal structure, microwave dielectric properties, 5G, resonators and antennas

1 Introduction

With the rapid development of 5G technology, there is an urgent need for high-performance microwave dielectric ceramics (Ohsato, 2005; Sebastian et al., 2015). As we enter the 5G communication era, microwave devices—an essential component of modern wireless communication systems—are expected to be lightweight and integrated (Yang et al., 2019; Zhang et al., 2021; Chen et al., 2023). The rapid technological progress in high-frequency electronics and communication systems has driven the ongoing quest for dielectric ceramic materials with exceptional microwave dielectric properties. These ceramics are crucial in various modern applications, including wireless communication systems, radar technology, satellite communications, and the emerging field of 5G telecommunications (Nomura, 1983; Reaney and Iddles, 2006; Huang et al., 2024). When considering practical applications like dielectric resonators, filters, duplexers, and waveguides in Microwave Dielectric Ceramics (MWDCs), it is essential to emphasize certain key parameters: i) Achieving a near-zero temperature coefficient of the resonant frequency to ensure temperature stability, ii) attaining a high-quality factor to minimize signal attenuation, and iii) maintaining an appropriate relative

permittivity (Nomura, 1983; Wersing, 1996; Ohsato, 2005; Reaney and Iddles, 2006; Sebastian and Jantunen, 2008; Liao et al., 2012; Xiang et al., 2018; Zhou et al., 2018; Yang et al., 2019; Zhang et al., 2021; Chen et al., 2023; Huang et al., 2024). M. T. Sebastian has also highlighted the potential practical applications of various dielectric ceramics (Sebastian, 2008). Within this overarching quest, the intriguing category of Wolframite-structured ceramics has emerged as a focal point of research, due to their unique crystal structures and the promise they hold in terms of exhibiting remarkable microwave dielectric properties. Among the various kinds of dielectric ceramics exhibiting low ε_r and high $Q \times f$ values, compounds from the rutile-like structural $M^{2+}M^{4+}Nb_2O_8$ family, with a monoclinic wolframite crystal structure, have shown remarkable microwave dielectric properties (Liao et al., 2012; Ramarao and Murthy, 2013; Li et al., 2015; Li et al., 2016; Wu and Kim, 2016).

Recently, these wolframite-structured ceramics, particularly ZnZrNb2O8, have garnered considerable attention due to their notable microwave dielectric properties (Liao et al., 2012; Ramarao and Murthy, 2013; Li et al., 2015; Li et al., 2016; Wu and Kim, 2016). In the wolframite crystal structure of $ZnZrNb_2O_8$, the Zn^{2+}/Zr^{4+} cations at the A-site occupy the 2*f* Wyckoff positions, while the Nb cations at the B-site reside in the 2*e* Wyckoff positions. Moreover, there are two distinct oxygen anions, O1 and O2, that occupy the 4 *g* Wyckoff positions. O1 is coordinated with two Zn^{2+}/Zr^{4+} cations and one Nb^{5+} cation, whereas O2 is bonded with one Zn^{2+}/Zr^{4}+ cation and two Nb^{5+} cations. Liao et al. were the first to report the microwave dielectric properties of $ZnZrNb_2O_8$ ceramics, noting a dielectric constant ε_r of 30, a quality factor $Q \times f$ of 61,000 GHz, and a temperature coefficient of resonant frequency τ_f of −52 ppm/°C (Liao et al., 2012). Subsequent research aimed on improving the $Q \times f$ value by substituting Zn with Mg, resulting in the formation of a solid solution, $MgZrNb_2O_8$. This new ceramic exhibited an $\varepsilon_r = 26$, $Q \times f = 120{,}816$ GHz, and $\tau_f = -50.2$ ppm/°C (Cheng et al., 2013), although it required sintering temperatures as high as 1,360°C. Ramarao and Murthy (2013) investigated the dielectric properties of other related ceramics, such as $MnZrNb_2O_8$ and $CoZrNb_2O_8$. The $MnZrNb_2O_8$ showed an $\varepsilon_r = 16.7$, $Q \times f = 40{,}700$ GHz, and $\tau_f = -29.6$ ppm/°C, while the $CoZrNb_2O_8$ ceramic demonstrated an $\varepsilon_r = 12.3$, $Q \times f = 26{,}950$ GHz, and $\tau_f = -28.2$ ppm/°C. Both materials exhibited relatively low dielectric constants and markedly decreased $Q \times f$ values. Li et al. synthesized $ZnZrNb_2O_8$ and $Zn_{0.95}M_{0.05}ZrNb_2O_8$ (M = Ni, Mg, Co, and Mn) ceramics at 1,280°C showed single-phase monoclinic structure and found that dielectric properties are correlated with density and polarizability, $Q \times f$ values increasing with packing fraction while τ_f shifting positively due to increased B-site bond valence (Li et al., 2015). Liu et al. investigated a new microwave dielectric ceramic $Zn_2V_2O_7$ with low sintering temperature and possessed optimum microwave dielectric properties of εr = 9.67, $Q \times f = 23{,}968$ GHz and $\tau_f = -19.87$ ppm/°C (Cao et al., 2022). Wang et al. (2018) similarly reviewed the recent development and advancement in the $A_2B_2O_7$ system (Wang et al., 2018).

$ZnZrNb_2O_8$ microwave dielectric ceramics are notable for their high $Q \times f$ values and relatively low sintering temperatures, boasting properties of $\varepsilon_r = 26.00$, $Q \times f = 65{,}000$ GHz, and $\tau_f = -54$ ppm/°C at a sintering temperature of 1,240°C (Huang et al., 2022), these characteristics make them promise for low-temperature co-fired ceramics (LTCC) technology applications. However, its inherently high sintering temperature (1,240°C) poses a limitation for their broader application in LTCC technology. Research continues actively in the pursuit of new ceramics, driven by the significant need for a diverse range of materials exhibiting different dielectric constants and high $Q \times f$ values.

Inspired by the existing literature, a key focus of current research is on reducing the sintering temperature of $ZnZrNb_2O_8$ ceramics while preserving their excellent microwave dielectric properties to unlock their potential for future material applications. This work undertakes a thorough exploration of $ZnZrNb_2O_8$ oxide ceramics, examining both their structural characteristics and microwave dielectric properties, which were synthesized via a solid-state reaction method. Our primary objective is to understand the complex relationship between the crystallographic features of $ZnZrNb_2O_8$ ceramics and their microwave dielectric performance. Additionally, we aimed to lower the sintering temperature of these ceramics without compromising their microwave dielectric properties.

2 Experimental procedures

2.1 Materials synthesis

The wolframite-structured $ZnZrNb_2O_8$ powders were synthesized via a solid-state reaction method by mixing the raw materials in accordance with the desired stoichiometry. The starting materials, namely ZnO (99.9%), ZrO_2 (99.0%), and Nb_2O_5 (99.9%), were utilized as high-purity oxide powders. To achieve homogeneity, the mixed powders were subjected to grinding for 4–5 h. Following this, the homogeneous mixtures were dried and calcined at 1,100°C for 4 h in a muffle furnace followed by another grinding for another 4–5 h. Then after, the resulting powders were then mixed with polyvinyl alcohol, acting as a binder, and subsequently granulated and pressed into cylindrical pellets of 10 mm diameter and approximately 5 mm in height. These pellets were initially preheated at a temperature of 600°C for 4 h to eliminate the binder. Finally, pelleted samples were preheated at 500°C for 4 h to fire the binder and sintered in the temperature range of 1,000°C–1,200°C for 4 h at a heating rate of 5°C/min. This specific heating rate was chosen to achieve the optimum sintering temperature for $ZnZrNb_2O_8$, resulting in nearly complete densification of the material.

2.2 Characterizations

The crystalline structure and phase of sintered samples were carried out by X-ray diffraction (Rigaku Ultima IV) utilizing Cu-Kα radiation, which was scanning in the 2θ range of 20°–80° with a scanning speed of 5°/min with steps of 0.02° under the settings of 40 kV and 40 mA. The dried samples were coated with gold, and its microstructures of the materials were recorded by a Quanta FEG 250 SEM system (FEI, Columbia, SC, United States). The apparent density of the $ZnZrNb_2O_8$ ceramics was calculated according to the Archimedes method using distilled water as the buoyancy medium.

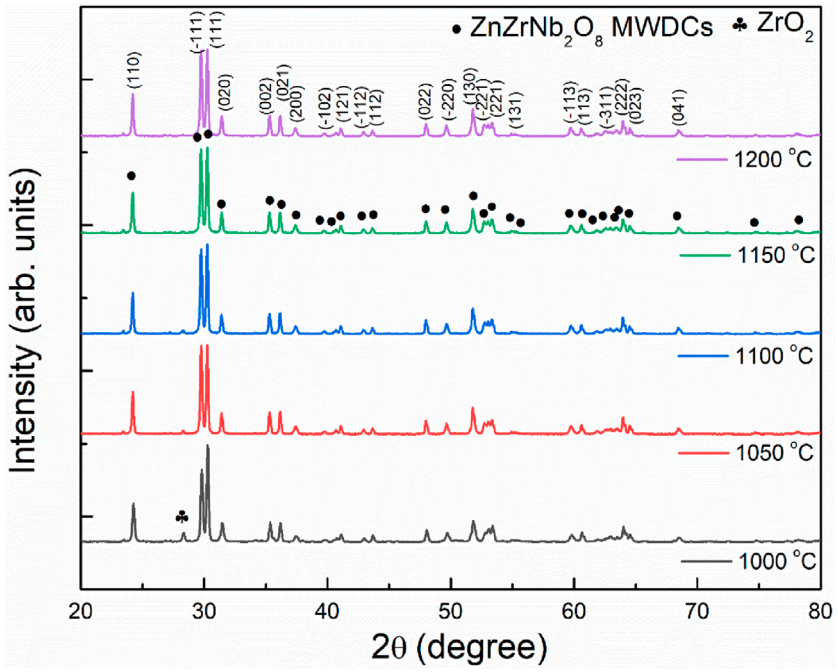

FIGURE 1
XRD patterns of $ZnZrNb_2O_8$ ceramics sintered at 1,000°C–1,200°C.

TABLE 1 Structural parameters (a, b, c), volume (V), bulk density (B.D.), relative density (R.D.) of $ZnZrNb_2O_8$ ceramics sintered at 1,000°C–1,200°C.

Sample (°C)	*a* (Å)	*b* (Å)	*c*(Å)	V(Å^3)	B.D. (g/cm^3)	R.D. (%)
1,000	4.8177	5.7045	5.0858	139.91	4.528	81.122
1,050	4.8165	5.7015	5.0835	139.58	4.810	86.174
1,100	4.8098	5.6993	5.0799	139.22	5.250	94.057
1,150	4.8025	5.6965	5.0786	139.15	5.537	99.199
1,200	4.8112	5.7117	5.0811	139.98	5.500	98.536

The theoretical density was calculated from the atomic weight and crystal structure by Eq. 1 (Xia et al., 2016):

$$\rho_{theory} = \frac{ZA}{V_C N_A} \tag{1}$$

where Z is the number of atoms in a unit cell, A is the atomic weight (g/mol), V_c is the volume of a unit cell (cm^3), N_A is Avogadro number (mol^{-1}). The relative density was calculated by Eq. 2:

$$\rho_{relative} = \frac{\rho_{bulk}}{\rho_{theory}} \tag{2}$$

A network analyzer (E5063A, Agilent Co., America) was used to measure the microwave dielectric properties of $ZnZrNb_2O_8$ ceramics. The dielectric constants are measured using the Hakki-Coleman method under $TE_{\delta 11}$ resonant mode (Courtney, 1970). The unloaded quality factors are measured by the cavity method (Kajfez et al., 1999). All measurements were operated at room temperature and in the frequency of 6–11 GHz. The calculation of τ_f is done using Eq. 3:

$$\tau_f = \frac{f_2 - f_1}{f_1 \Delta T} \tag{3}$$

where f_2 and f_1 represented the resonant frequencies at temperature of T_2 and T_1, respectively and measured in the temperature range of 25°C–85°C.

The Hakki-Coleman method is a widely used technique for the characterization of dielectric resonators and is often employed to decide the complex permittivity ε_r of materials. It involves measuring the resonant frequency (f_r) and the unloaded quality factor (Q_u) of a dielectric resonator and using these values to calculate the complex permittivity. Eq. 4 is associated with the Hakki-Coleman method:

Resonant Frequency (fr):

$$f_r = \frac{c}{2\pi\sqrt{\varepsilon_r}} \tag{4}$$

where (c) is the speed of light in vacuum, and (εr) is the relative permittivity of the material.

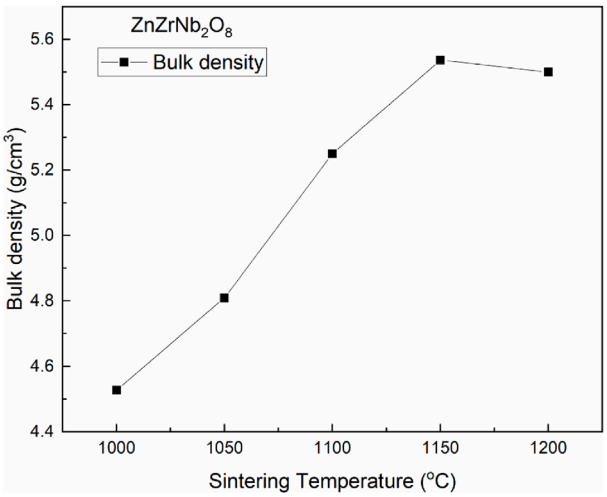

FIGURE 2
The variation of apparent density of $ZnZrNb_2O_8$ ceramics sintered at different temperatures.

Quality factor (Q_u) was measured according to Eq. 5:

$$Q_u = \frac{f_r}{\Delta f} \tag{5}$$

where (Δf) is the bandwidth below the resonant peak.

Complex Permittivity (ε_r) was measured according to Eq. 6:

$$\varepsilon_r = \frac{c}{2\pi f_r Z_0 Q_u} \tag{6}$$

where (Z_0) is the characteristic impedance of free space ($Z_0 = 377\ \Omega$).

These equations allow for the calculation of the complex permittivity (ε_r) of a material based on experimental measurements of resonant frequency (fr) and unloaded quality factor (Q_u).

3 Results and discussions

Figure 1 represents the X-ray diffraction (XRD) patterns of $ZnZrNb_2O_8$ ceramics sintered within the temperature range of 1,000°C–1,200°C for a duration of 4 h. The XRD analysis reveals that all the ceramics exhibit a solid phase characterized by a monoclinic wolframite structure with the *P2/c* space group. The observed XRD peaks were matched well with the standard data (JCPDS PDF #48-0324). Notably, the higher sintering temperatures lead to the elimination of the ZrO_2 phase. The calculated parameters for $ZnZrNb_2O_8$ sintered at 1,150°C are as follows: a = 4.8025 Å, b = 5.6965 Å, c = 5.0786 Å, and V = 139.15 Å^3. The structural parameters, cell volume, bulk density, and relative density were summarized in Table 1. We observed that with the increase in sintering temperature, the lattice parameters and cell volume decreased at first and then increased.

In Figure 2, the correlation between apparent densities and sintering temperature in $ZnZrNb_2O_8$ ceramics is evident. The apparent densities of the samples consistently increased with the rising sintering temperatures, peaking between 1,150°C and 1,200°C. This indicates that $ZnZrNb_2O_8$ ceramics can attain nearly full density when sintered within this temperature range. Furthermore, Figure 3 presents SEM images of $ZnZrNb_2O_8$ ceramics sintered at temperatures ranging from 1,000°C to 1,200°C. As depicted in Figures 3A–D, grain size becomes more pronounced with higher sintering temperatures. It was evident from Figure 3A that there was some porosity, indicating that the $ZnZrNb_2O_8$ ceramic sintered at 1,000°C was not dense. With increasing sintering temperatures, grain development was observed. At 1,150°C, the grains were uniform and dense, with nearly eliminated porosity, as seen in Figure 3C. Higher sintering temperatures promote grain growth and a more uniform grain distribution. Larger grains reduce grain boundary effects and enhance polarization, leading to an increase in dielectric constant. However, at 1,200°C, a somewhat uneven distribution of grain size was noticed, causing non-uniform grain development, a little reduction in density, and a deterioration of the sample's dielectric properties. The microstructures of $ZnZrNb_2O_8$ ceramics exhibit high density and uniformity, with minimal pores, and an average grain size of 2.5 μm.

Figure 4 demonstrates the variations in dielectric constant (ε_r), quality factor (Qxf), and thermal coefficient of resonant frequency (τ_f) in $ZnZrNb_2O_8$ ceramics as sintering temperatures vary. The dielectric constant is usually influenced by both extrinsic factors like density, porosity, grain size and distribution, grain boundaries, and secondary phases, as well as intrinsic parameters such as polarizability and structural characteristics (Guo et al., 2011; Huan et al., 2013; Song et al., 2014; Cao et al., 2015). As sintering temperature increases, the densification of the ceramic materials occurs due to enhanced diffusion and particle rearrangement, leading to reduced porosity and increased density, consequently elevating the dielectric constant. Higher sintering temperatures aid in eliminating secondary phases and promoting grain boundary migration, thereby enhancing dielectric properties.

Conversely, lower temperatures may result in limited polarization and incomplete densification, affecting dielectric constant values. Enhanced polarization with increasing sintering temperature leads to higher dielectric constant values. Changes in the lattice parameters occur during sintering, affecting the material's dielectric properties. Optimal sintering temperature results in a well-defined crystal structure, maximizing polarization and dielectric constant. In this work, the dielectric constant reaches its optimization point at a specific sintering temperature (e.g., 1,150°C), where density, grain size, and polarization effects are maximized, as depicted in Figure 4 and Table 2. However, beyond this optimal temperature, further increases in sintering temperature may lead to adverse effects such as grain coarsening, excessive grain growth, or formation of secondary phase, causing a decline in the dielectric constant due to decreased polarization efficiency and increased defects. Additionally, certain resonant frequency values for ε_r are indicated in Figure 4., which align with changes in apparent density and are primarily driven by the sample density, grain size, and polarization characteristics (Huang et al., 2023).

To assess the structural dependency of the dielectric constant, the observed dielectric polarizability ($\alpha_{obs.}$) was calculated and compared to the theoretical dielectric polarizability ($\alpha_{theo.}$). Based on the Clausiuse–Mosotti equation, we used the Eq. 7 to calculate the $\alpha_{obs.}$ (Shannon, 1993):

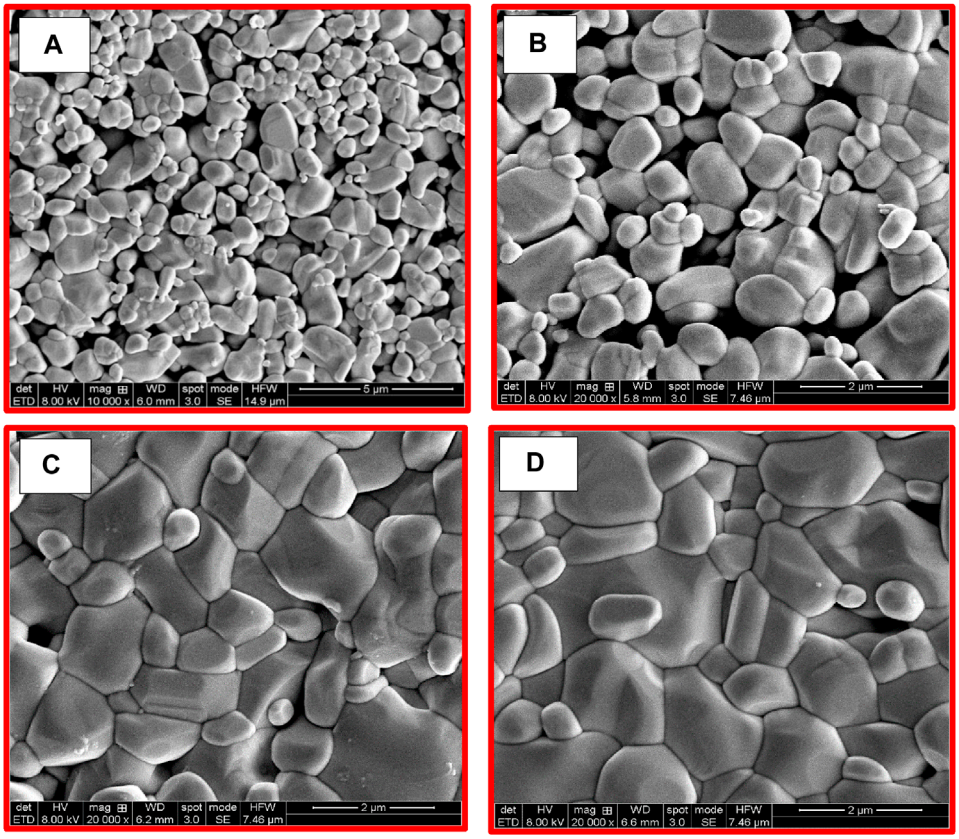

FIGURE 3
Surface morphologies of $ZnZrNb_2O_8$ ceramics sintered at **(A)** 1,000°C; **(B)** 1,100°C; **(C)** 1,150°C; **(D)** and 1,200°C.

$$\alpha_{obs.} = \frac{1}{b} V_m \frac{(\varepsilon - 1)}{(\varepsilon + 2)} \tag{7}$$

where, ε is the measured dielectric constant; b is 4π/3, and V_m is molar volume, respectively.

And theoretical dielectric polarizability ($\alpha_{theo.}$) of the samples was calculated by additive rule of molecular polarizability shown in Eq. 8 (Shannon and Rossman, 1992):

$$\alpha_{theo.}(ZnZrNb_2O_8) = \alpha_D(Zn^{2+}) + \alpha_D(Zr^{4+}) + 2\alpha_D(Nb^{5+}) + 8\alpha_D(O^{2-}) \tag{8}$$

where, $\alpha(Zn^{2+})$, $\alpha(Zr^{4+})$, $\alpha(Nb^{5+})$, and $\alpha(O^{2-})$ represented ions polarizabilities reported by Shannon (Shannon, 1993). The calculated values of $\alpha_{obs.}$and $\alpha_{theo.}$ are documented in Table 2. By comparison, it could be found $\alpha_{theo.}$ and $\alpha_{obs.}$ values were in good agreement with each other and the deviation from the $\alpha_{obs.}$ and $\alpha_{theo.}$ could be attributed to relative density because of the $\alpha_{obs.}$ values depended on specimens and fabrication process.

Subsequently, the $Q \times f$ values at various sintering temperatures and their respective resonant frequencies are shown in the middle section of Figure 4 and observed values are presented in Table 2. At lower sintering temperatures (below 1,150°C), the increase in $Q \times f$ values are attributed to the reduction in porosity. As the temperature rises, particles within the ceramic compact bond more effectively, resulting in enhanced densification and reduced porosity, which in turn increases the $Q \times f$ values. However, when the sintering temperature exceeds 1,150°C, a slight decrease in $Q \times f$ values is observed. This decline in $Q \times f$ values can be attributed to changes in the crystal structure or its parameters. Thus, excessive sintering temperatures may cause grain growth and phase transformations, altering the crystal lattice and electrical properties of the material. The trend of an initial increase followed by a subsequent decline after reaching the optimal value suggests an ideal sintering temperature range for maximizing $Q \times f$ values. At lower temperatures, porosity reduction predominates, as evidenced by the SEM images in Figure 3, leading to increase in $Q \times f$ values, while at higher temperatures, changes in structural parameters become more influential, eventually causing a decline in $Q \times f$ values beyond the optimal sintering temperature range.

It has been documented that dielectric loss in the microwave frequency range is associated with the packing fraction of the structure (Cao et al., 2015). Similarly, Liao et al. (2012) have observed that changes in the quality factor correlate with the compound's packing fraction. To elucidate the changes in the quality factor of $ZnZrNb_2O_8$ ceramics, the packing fraction was calculated using the following Eq. 9:

$$\begin{aligned} Packing\,Fraction\,(\%) &= \frac{Volume\,of\,atoms\,in\,the\,cell}{Volume\,of\,primitive\,unit\,cell} \\ &= \frac{\frac{4\pi}{3} \times \left(r_{Zn}^3 + r_{Zr}^3 + 2 \times r_{Nb}^3 + 8 \times r_o^3\right)}{Volume\,of\,unit\,cell} \times Z \end{aligned} \tag{9}$$

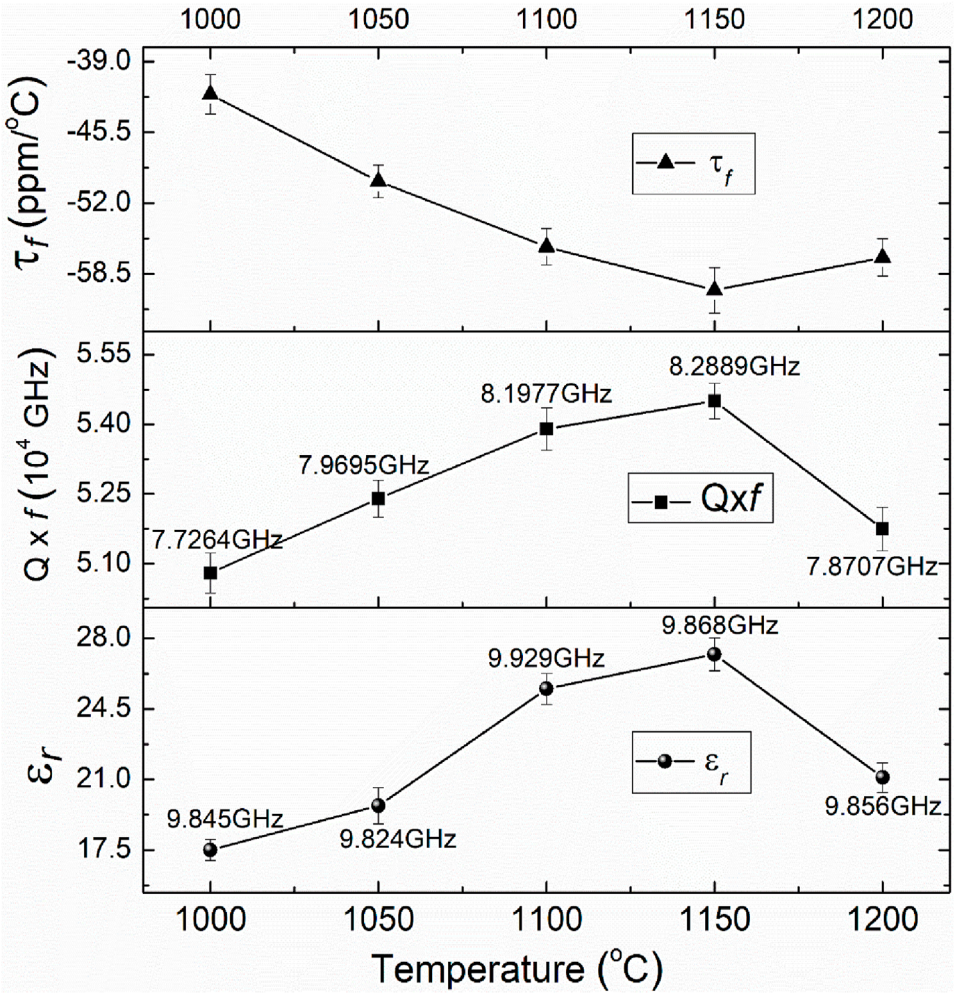

FIGURE 4
Variation of dielectric constant, Q × *f* value, and temperature coefficient of resonant frequency (τ*f*) with sintering temperature. In the figure, certain resonance frequency values for dielectric constant and Q × *f* are indicated.

TABLE 2 The dielectric polarizabilities, dielectric constant, packing fraction and Q × *f* value of of $ZnZrNb_2O_8$ ceramics sintered at 1,000°C–1,200°C.

Sample (°C)	αtheo	εr	αobs	P.F. (%)	Q × f (GHz)	τf (ppm/°C)
1,000	29.31	17.5	20.99	63.96	50,800	−42
1,050	29.31	19.7	20.12	64.31	52,400	−50
1,100	29.31	25.5	19.06	64.78	53,900	−56
1,150	29.31	27.2	18.20	64.85	54,500	−60
1,200	29.31	21.1	17.77	64.41	51,750	−57

where, r_{Zn}, r_{Zr}, r_{Nb} and r_O represent the ionic radii of the Zn^{2+}, Zr^{4+}, Nb^{5+} and O^{2-}, respectively. Z is the number of formula units per unit cell.

The decrease in packing fraction, as detailed in Table 2, resulted in increased lattice vibrations and non-harmonic vibrations. This, in turn, caused a decline in the Q × *f* values when the sintering temperatures ranged from 1,150°C to 1,200°C.

To understand the observed trend in the temperature coefficient of resonant frequency (τ_f) in relation to the sintering temperature for $ZnZrNb_2O_8$ ceramics, it is essential to consider the microstructural changes occurring during the sintering process and their impact

on the material's properties. Figure 4 (upper part) illustrates the τ_f values at different sintering temperatures. The variations in τ_f can be explained by the changes in the ceramic's crystal structure, grain size, and density as the material is subjected to different sintering temperatures. As the sintering temperature rises, the grains in the ceramic material can enlarge, leading to an increase in the ceramic's density by reducing its porosity. The size of these grains influences the dielectric properties, which in turn can alter the resonant frequency and its temperature coefficient of resonant frequency.

At lower sintering temperatures (1,000°C–1,050°C), densification is incomplete, and grain growth is limited, leading to a relatively porous microstructure with smaller grain sizes. Therefore, the microwave properties are not optimized, resulting in higher τ_f values. As the sintering temperature increases to 1,100°C–1,150°C, densification improves, and grain growth becomes more significant. The increased density and larger grain size enhance the microwave properties, resulting in lower τ_f values. However, sintering at higher temperatures (around 1,200°C) may lead to excessive grain growth and coarsening of the microstructure, which may degrade the microwave properties, causing an increase in τ_f. The observed trend, where τ_f initially decreases, reaches a minimum at 1,150°C, and then increases, suggests that the optimum sintering temperature range for achieving the best microwave properties, including a low τ_f value, is around 1,150°C. For the specific case of $ZnZrNb_2O_8$ ceramics sintered at 1,150°C for 4 h, the excellent microwave dielectric properties observed (ε_r = 27.2, $Q \times f$ = 54,500 GHz, and τ_f = −60 ppm/°C) indicate that this sintering condition produces an optimized microstructure and phase composition for microwave applications. These results are consistent with previously reported data by Wang et al. (2023).

4 Conclusion

In this study, we explored the impact of sintering temperature on both the microstructure and microwave dielectric properties of $ZnZrNb_2O_8$ ceramics. Using the solid-state method, we successfully obtained $ZnZrNb_2O_8$ microwave dielectric ceramics and systematically investigated their microwave properties depending in relation to varying sintering temperatures. The structure of $ZnZrNb_2O_8$ ceramics remained consistent across different temperatures, as revealed by XRD results indicating the formation of the monoclinic wolframite structure in the $ZnZrNb_2O_8$ phase. Notably, the relative density played a significant role in influencing the dielectric constant and other microwave dielectric parameters. Specifically, the $ZnZrNb_2O_8$ ceramic sintered at 1,150°C exhibited promising characteristics, including a dielectric constant (ε_r) of 27.2, a quality factor ($Q \times f$) of 54,500 GHz, and a temperature coefficient of frequency (τ_f) of −60 ppm/°C. These findings suggest the potential application of these ceramics in microwave components.

Data availability statement

The original contributions presented in the study are included in the article/supplementary material, further inquiries can be directed to the corresponding author.

Author contributions

AK: Conceptualization, Data curation, Formal Analysis, Funding acquisition, Investigation, Methodology, Project administration, Resources, Validation, Visualization, Writing–original draft, Writing–review and editing. PS: Formal Analysis, Funding acquisition, Investigation, Resources, Validation, Visualization, Writing–review and editing. QF: Funding acquisition, Resources, Visualization, Writing–review and editing.

Funding

The author(s) declare that financial support was received for the research, authorship, and/or publication of this article. This research was funded by the High-end Foreign Experts Introduction Program of Ministry of Science and Technology of China Project (grant number: G2022036014L), Luzhou Municipal Science and Technology Plan Project (grant numbers: 2021-JYJ-98, 2021-JYJ-99), and Department of Science and Technology of Sichuan province Key R&D research Program (grant number 22ZDYF3765).

Conflict of interest

The authors declare that the research was conducted in the absence of any commercial or financial relationships that could be construed as a potential conflict of interest.

Publisher's note

References

Cao, Z. Z., Wang, L. Y., He, W. Y., Zeng, J. T., Gao, Y. F., Liu, J. R., et al. (2015). The electric and dielectric responses of $La_2Ni_{1-x}Mg_xMnO_6$ solid solution. *J. Alloys Compd.* 628, 81–88. doi:10.1016/j.jallcom.2014.12.051

Cao, H., Chen, L., and Li, B. (2022). A new microwave dielectric ceramic $Zn_2V_2O_7$with low sintering temperature. *Mater. Lett.* 326, 132924. doi:10.1016/j.matlet.2022.132924

Chen, X., Guan, Y., Zhong, Z., Wang, F., Li, W., Mao, H., et al. (2023). Effect of Zr^{4+} substitution on the phase evolution and microwave dielectric properties of $(Cu_{1/3}Nb_{2/3})_{0.25}Ti_{0.75-x}Zr_x$ O_2 ceramics. *Ceram. Int.* 49, 5022–5028. doi:10.1016/j.ceramint.2022.10.015

Cheng, Y., Zuo, R. Z., and Lv, Y. (2013). Preparation and microwave dielectric properties of low-loss MgZrNb2O8 ceramics. *Ceram. Int.* 39, 8681–8685. doi:10.1016/j.ceramint.2013.04.048

Courtney, W. E. (1970). Analysis and evaluation of a method of measuring the complex permittivity and permeability microwave insulators. *IEEE Trans. Microw. Theory Tech.* 18, 476–485. doi:10.1109/tmtt.1970.1127271

Guo, M., Gong, S. P., Dou, G., and Zhou, D. (2011). A new temperature stable microwave dielectric ceramics: ZnTiNb2O8 sintered at low temperatures. *J. Alloy. Compd.* 509, 5988–5995. doi:10.1016/j.jallcom.2011.01.095

Huan, Z. L., Sun, Q. C., Ma, W. B., Wang, L., Xiao, F., and Chen, T. (2013). Crystal structure and microwave dielectric properties of (Zn1−xCox)TiNb2O8 ceramics. *J. Alloy. Compd.* 551, 630–635. doi:10.1016/j.jallcom.2012.11.072

Huang, Z., Li, L., and Qiao, J. (2022). Trace additive enhances microwave dielectric performance significantly to facilitate 5G communications. *J. Am. Ceram. Soc.* 105, 7426–7437. doi:10.1111/jace.18688

Huang, Z., Qiao, J., and Li, L. (2023). Structural characteristics and microwave dielectric performances of ZnZrNb2-xVx/2O8-1.25x-based ceramics for LTCC applications. *Ceram. Int.* 49, 31524–31529. doi:10.1016/j.ceramint.2023.07.103

Huang, Z., Qiao, J., and Li, L. (2024). Microwave dielectric ceramics with low dielectric loss and high temperature stability for LTCC applications. *Ceram. Int.* 50 (6), 9029–9033. doi:10.1016/j.ceramint.2023.12.216

Kajfez, D., Chebolu, S., Abdul-Gaffoor, M. R., and Kishk, A. A. (1999). *Microw. Theory Tech.* 27, 367–371.

Li, L. X., Sun, H., Cai, H. C., and Lv, X. S. (2015). Microstructure and microwave dielectric characteristics of ZnZrNb2O8 and (Zn0.95M0.05)ZrNb2O8 (M = Ni, Mg, Co and Mn) ceramics. *J. Alloy. Compd.* 639, 516–519. doi:10.1016/j.jallcom.2015.03.001

Li, L. X., Zhang, S., Ye, J., Lv, X. S., Sun, H., and Li, S. (2016). Crystal structure and microwave dielectric properties of the low dielectric loss ZnZr1−Sn Nb2O8 ceramics. *Ceram. Int.* 42, 9157–9161. doi:10.1016/j.ceramint.2016.03.006

Liao, Q. W., Li, L. X., Ren, X., Yu, X. X., Guo, D., and Wang, M. J. (2012). A low sintering temperature low loss microwave dielectric material $ZnZrNb_2O_8$. *J. Am. Ceram. Soc.* 95 (11), 3363–3365. doi:10.1111/j.1551-2916.2012.05450.x

Nomura, S. (1983). Ceramics for microwave dielectric resonator. *Ferroelectrics* 49, 61–70. doi:10.1080/00150198308244666

Ohsato, H. (2005). Research and development of microwave dielectric ceramics for wireless communications. *J. Ceram. Soc. Jpn.* 113, 703–711. doi:10.2109/jcersj.113.703

Ramarao, S. D., and Murthy, V. R. K. (2013). Crystal structure refinement and microwave dielectric properties of new low dielectric loss AZrNb2O8 (A: Mn, Zn, Mg and Co) ceramics. *Scr. Mater.* 69, 274–277. doi:10.1016/j.scriptamat.2013.04.018

Reaney, I. M., and Iddles, D. (2006). Microwave dielectric ceramics for resonators and filters in mobile phone networks. *J. Am. Ceram. Soc.* 89, 2063–2072. doi:10.1111/j.1551-2916.2006.01025.x

Sebastian, M. T. (2008). *Dielectric materials for wireless communication*. Amsterdam, Netherlands: Elsevier Science.

Sebastian, M. T., and Jantunen, H. (2008). Low loss dielectric materials for LTCC applications: a review. *Int. Mater. Rev.* 53 (2), 57–90. doi:10.1179/174328008x277524

Sebastian, M. T., Ubic, R., and Jantunen, H. (2015). Low-loss dielectric ceramic materials and their properties. *Int. Mater. Rev.* 60, 392–412. doi:10.1179/1743280415y.0000000007

Shannon, R. D. (1993). Dielectric polarizabilities of ions in oxides and fluorides. *J. Appl. Phys.* 73, 348–366. doi:10.1063/1.353856

Shannon, R. D., and Rossman, G. R. (1992). *Am. Min.* 77, 94–100.

Song, Z. K., Zhang, P., Wang, Y., and Li, L. X. (2014). Improved quality factor of NdNbO4 microwave dielectric ceramic by Mn2+ substitution. *J. Alloys Compd.* 583, 546–549. doi:10.1016/j.jallcom.2013.09.023

Wang, G., Chen, Z., Yan, H., Xuan, T., Wu, M., Zhu, X., et al. (2023). Crystal structure, Raman spectra, and modified dielectric properties of pure-phase $ZnZrNb_2O_8$ ceramics at low temperature. *J. Am. Ceram. Soc.* 106, 1912–1920. doi:10.1111/jace.18892

Wang, Z., Zhou, G., Jiang, D., and Wang, S. (2018). Recent development of $A_2B_2O_7$ system transparent ceramics. *J. Adv. Ceram.* 7, 289–306. doi:10.1007/s40145-018-0287-z

Wersing, W. (1996). Microwave ceramics for resonators and filters. *Curr. Opin. Solid State Mater. Sci.* 1 (5), 715–731. doi:10.1016/s1359-0286(96)80056-8

Wu, H., and Kim, E. S. (2016). Characterization of crystal structure and microwave dielectric properties of AZrNb2O8 (A = Zn, Co, Mg, Mn) ceramics based on complex bond theory. *Ceram. Int.* 42 (5), 5785–5791. doi:10.1016/j.ceramint.2015.12.119

Xia, W.-S., Yang, F.-Y., Zhang, G.-Y., Han, K., and Guo, D.-c. (2016). New low-dielectric-loss NiZrNb 2 O 8 ceramics for microwave application. *J. Alloy. Compd.* 656, 470–475. doi:10.1016/j.jallcom.2015.10.008

Xiang, H., Li, C., Jantunen, H., Fang, L., and Hill, A. E. (2018). Ultralow loss $CaMgGeO_4$ microwave dielectric ceramic and its chemical compatibility with silver electrodes for low-temperature cofired ceramic applications. *ACS Sustain. Chem. Eng.* 6 (5), 6458–6466. doi:10.1021/acssuschemeng.8b00220

Yang, H., Zhang, S., Yang, H., Yuan, Y., and Li, E. (2019). Intrinsic dielectric properties of columbite $ZnNb_2O_6$ ceramics studied by P–V–L bond theory and Infrared spectroscopy. *J. Am. Ceram. Soc.* 102, 5365–5374. doi:10.1111/jace.16385

Zhang, Q., Huang, F., Su, H., Wu, X., Li, Y., and Tang, X. (2021). Effects of LiF addition on sintering characteristics and microwave dielectric properties of wolframite structure ZnWO4 ceramics. *Ceram. Int.* 47, 24809–24816. doi:10.1016/j.ceramint.2021.05.206

Zhou, D., Pang, L.-X., Wang, D.-W., Qi, Z.-M., and Reaney, I. M. (2018). High quality factor, ultralow sintering temperature $Li_6B_4O_9$ microwave dielectric ceramics with ultralow density for antenna substrates. *ACS Sustain. Chem. Eng.* 6 (8), 11138–11143. doi:10.1021/acssuschemeng.8b02755